The Florida control scheme

Guido Mueller, Tom Delker, David Reitze, D. B. Tanner
Department of Physics, University of Florida,
Gainesville 32611-8440, Florida, USA

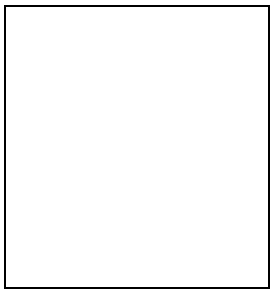

The most likely configuration for the second generation of large-scale gravitational-wave detectors like the LIGO-detector will be a dual-recycled cavity-enhanced Michelson interferometer. The main problem of this configuration is to find a possible control scheme for all longitudinal degrees of freedom. Our group has designed the first frontal modulation locking scheme which is capable to lock all 5 longitudinal degrees of freedom.

1 Introduction

In recent years, several large scale gravitational wave detectors have been designed and are now under construction. The Japanese 300 m TAMA-detector [1], the French-Italian 3 km VIRGO-detector [1] and the three US-LIGO-detectors [1] (2 km and 4 km in Hanford, WA and 4 km in Livingston, LA) will all be cavity enhanced Michelson interferometers with power recycling. The German-British 600 m GEO600 detector [1] will be a signal- and power-recycled delay-line Michelson interferometer. All these detectors may reach a sensitivity high enough to detect for the first time gravitational waves. Nevertheless, without further improvements many very interesting sources of gravitational waves cannot be detected.
In addition to mirrors and beamsplitters with lower absorption rates, improved suspension systems, and a laser source with more output power, the most likely improvement for the LIGO detector is an additional mirror at the dark port (see fig. 1). This optical layout is called signal recycling or, if applied with power recycling, dual recycling. A primary reason why dual recycling is not being installed in the LIGO-detector in the first place is the control problem of the longitudinal degrees of freedom. Thus far, control schemes have been tested for cavity enhanced Michelson interferometers with power recycling [2] and for dual recycled Michelson interferometers without cavities [3] in the arms. It is the aim of our work to tailor a possible control scheme, a

sensible readout scheme, and to examine various other aspects of this kind of interferometer.

2 Dual recycled cavity enhanced Michelson interferometer

A dual recycled cavity enhanced Michelson interferometer is an optical setup which combines 5 optical resonators and 2 Michelson interferometers (see fig. 1).

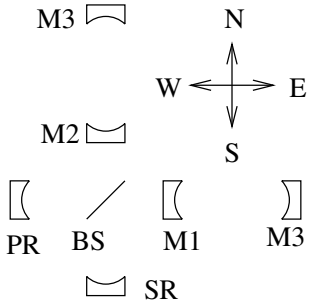

Figure 1: Dual-recycled cavity-enhanced Michelson interferometer.

In its centre it has a beamsplitter (BS) which defines the four directions *North, East, South, West*. The light from the laser impinges first on the power recycling (PR) mirror, which is placed in the west arm of the interferometer. The light transmitted through the PR-mirror is divided into two beams at the beamsplitter. These two beams are coupled into the arm cavities of the north and the east arm. The return fields from the cavities are superimposed at the beamsplitter again. We will refer to this first Michelson interferometer (MI1) as "dark" if most of the light is send back into the west arm and as"bright" if most of the light is sent into the south arm. A "dark" MI1, together with the PR-mirror, forms the power recycling cavity (PR-cavity).

The light which propagates to the south arm will be reflected back at the SR-mirror. This light will interfere with the incoming light at the beamsplitter. This second Michelson interferometer alters the reflectivity and the transmissivity of the beamsplitter and can lead to a strange asymmetric field distribution in the North and the East arm. The SR-mirror and a "dark" first Michelson forms the signal recycling cavity (SR-cavity). If the Michelson is "bright" the SR-mirror together with MI1 and the PR-mirror forms the signal recycling power recycling cavity (SR-PR-cavity).
Altogether we have 5 different cavities and 2 Michelson interferometers or 7 longitudinal degrees of freedom; these are not independent. If for example the SR-cavity and the PR-cavity are both resonant with the incoming field then is the SR-PR-cavity also resonant. Also, the length of the SR-cavity is not independent of the interference of MI2. This reduces the number of independent longitudinal degrees of freedom to 5.
There are several different possible basis for describing the state of the interferometer. We will use the following set of degrees of freedom:
1. Common Fabry Perot mode: The average length of the two arm cavities with respect to the incoming light field.
2. Differential Fabry Perot mode: The length of the two arm cavities with respect to each other.
3. Differential MI1 mode: The length of the *short* north arm (BS to M2) with respect to the short east arm (BS to M1).
4. PR cavity: The length of the PR-cavity with respect to the incoming light field.
5. SR-PR cavity: The length of the SR-PR-cavity with respect to the incoming light field.

The alteration of the space time metric due to the gravitational wave will alter the length of the two arm cavities with respect to each other (differential Fabry Perot mode). This degree of freedom senses the gravitational waves and must be measured with extreme sensitivity. This measurement can be done when the main frequency component (the carrier) of the light field is resonant within both arm cavities, is "dark" in the first Michelson, and is resonant within the PR-cavity.
A small difference in the differential Fabry Perot mode relative to the working point alters the

interference of the first Michelson interferometer. It will not be perfectly dark anymore; a small amount of the carrier will be sent to the dark port. The amplitude of this light is proportional to the amplitude of the difference whereas the sign depends on the sign of the difference.
A gravitational wave will modulate the phase of the light inside the arm cavities. This modulation will generate sidebands relative to the carrier with a frequency spectrum equal to the frequency spectrum of the gravitational wave. These sidebands will propagate in the arm cavities. If their frequencies are within the linewidth of the cavities, they will experience a build up of their intensity. Otherwise, the cavity will average over the whole gravitational wave and the sidebands will be suppressed by the cavities. The bandwidth of a detector without signal recycling is only determined by the linewidth of the arm cavities.
The first Michelson interferometer is bright for these sidebands because they are generated with opposite phases in both arms. Without a signal recycling mirror these sidebands are simply demodulated at the photodetector.
In a signal-recycled interferometer, the additional mirror at the dark port will reflect the sidebands back into the interferometer. But because the first Michelson interferometer is also dark from this side, the whole setup acts as a new cavity called the signal-recycling cavity.
This new cavity together with the average arm cavity forms a linear, three-mirror cavity. The behaviour of two coupled cavities sharing one mirror (here the first cavity mirror of the average arm cavity) is quite complicated. It can be understood if one sees the signal recycling cavity as a mirror with a frequency-dependent, complex reflectivity which depends on its length.
If the reflectivity of the signal recycling cavity at the signal frequency (carrier +/- GW-frequency) is high compared to the reflectivity of the first cavity mirror the effective finesse of the arm cavities will increase for this particular frequency. This high finesse increases the build up of the signal sideband at the new resonance frequency of the three mirror cavity but reduces the bandwidth of the whole interferometer. (See fig. 2.)

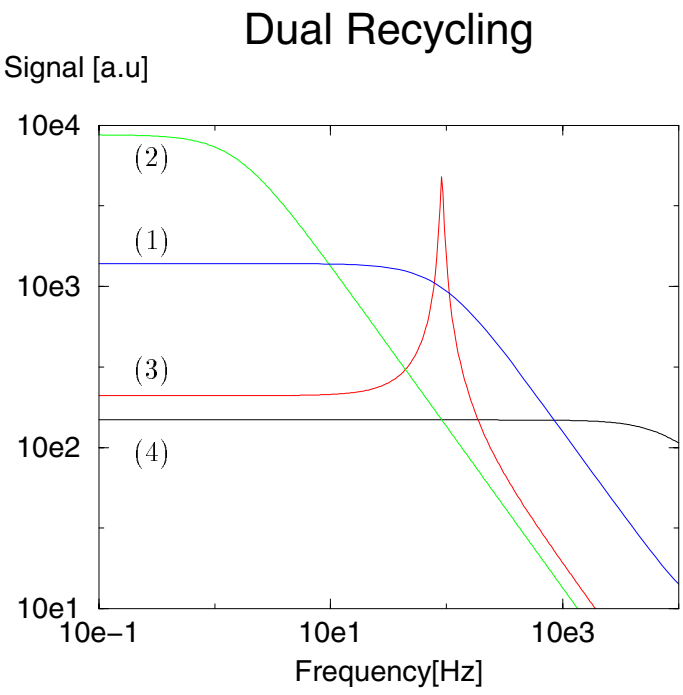

Figure 2: Signal strength for various configurations: (1) LIGO-I-configuration w/o dual recycling, (2) broadband dual recycling, (3) detuned dual recycling, (4) resonant sideband extraction.

Curve 1 shows the signal strength at the output of a gravitational wave detector without signal recycling mirror (LIGO-I configuration). In the case of broadband signal recycling the new resonance frequency is equal to the carrier frequency (curve 2). The signal can be significantly higher, but only for a smaller bandwidth. This setup is of particular interest for signals at low frequencies and for low-finesse arm cavities. Detuned signal recycling (curve 3) can increase the sensitivity at frequencies which even are above the linewidth of the arm cavities. Resonant sideband extraction reduces the effective reflectivity of the arm cavities and increases therefore the bandwidth of the detector (curve 4). It has no special peak sensitivity but, using high-finesse arm cavities, RSE can be used to build a broadband and very sensitive interferometer.

3 Modulation/Demodulation spectroscopy

We propose using two different modulation frequencies to generate the signals which are necessary to control all 5 longitudinal degrees of freedom. A laser field which is phase modulated with two modulation frequencies contains in first order five different frequency components:

$$E_{in} \approx E_o e^{i\omega_o t}\left(1 + \frac{m_1}{2}e^{i\Omega_1 t} - \frac{m_1}{2}e^{-i\Omega_1 t} + \frac{m_2}{2}e^{i\Omega_2 t} - \frac{m_2}{2}e^{-i\Omega_2 t}\right) \quad (1)$$

These five components will propagate independently through the interferometer. The field at one detector can then be calculated by multiplying every component with its own transfer function:

$$E_{det} = E_o e^{i\omega_o t}\left(T(0) + \frac{m_1}{2}T(\Omega_1)e^{i\Omega_1 t} - \frac{m_1}{2}T(-\Omega_1)e^{-i\Omega_1 t} + \frac{m_2}{2}T(\Omega_2)e^{i\Omega_2 t} - \frac{m_2}{2}T(-\Omega_2)e^{-i\Omega_2 t}\right) \quad (2)$$

The photodetector detects the intensity of the field. We are only interested in the parts which oscillate with the modulation frequencies:

$$\begin{aligned} I_{\Omega_i} \quad &= m_i E o^2 \quad [\Re(T(0)\,(T^*(\Omega_i) - T^*(-\Omega_i)))\cos(\Omega_i(t+\tau)) \\ &\quad +\Im(T(0)\,(T^*(\Omega_i) + T^*(-\Omega_i)))\sin(\Omega_i(t+\tau))] \end{aligned} \quad (3)$$

There are two signal parts, usually called the in-phase ($\propto \sin(\Omega_i(t+\tau))$) and the quadrature ($\propto \cos(\Omega_i(t+\tau))$) components. A pure in-phase signal appears when the dispersion (phase change) in the transfer function of the carrier is different from the dispersion in the transfer functions of the sidebands. A pure quadrature signal appears when the amplitudes of the transfer functions of the sidebands differ from each other. A mixture appears when the dispersion in the transfer functions of the sidebands are different from and not antisymmetric to each other.
The demodulated signal will be a linear combination of both signals. The mixing angle depends on the tunable phase of the RF local oscillator:

$$\begin{aligned} I_{mix} \quad &= A \quad [\Re(T(0)\,(T^*(\Omega_i) - T^*(-\Omega_i)))\cos(\alpha) && (4) \\ &\quad - \quad \Im(T(0)\,(T^*(\Omega_i) + T^*(-\Omega_i)))\sin(\alpha)] && (5) \end{aligned}$$

The goal of every locking scheme is to generate strong linear independent error signals for every degree of freedom, or at least enough linearly independent signals to lock the degrees of freedom gradually.

In addition, the intensity of the local oscillator has to be higher than the intensity of all other light (mainly stray light) on the detector at the dark port. Only in this case is the signal to shot noise ratio determined by the number of photons in the carrier at the beamsplitter and not by the number of photons in the stray light.

4 The Locking scheme

We chose the macroscopic lengths in such a way that the first Michelson is dark and the PR-cavity is slightly detuned for the Ω_1-sidebands. The first Michelson will be nearly bright and the PR-SR-cavity should be on resonance for the Ω_2-sidebands. The arm cavities are neither resonant nor anti-resonant with the sidebands. They will experience a small phase shift when they are reflected at the cavities. This phase change is necessary to keep the two modulation frequencies from being multiples of each other.
We plan to detect the control signals at three different ports (see fig. 3). The first will detect the reflected light in front of the PR-mirror, the second will pick off some light between beamsplitter

and PR-mirror, and the last one the through coming signal behind the SR-mirror.
A common change of the arm cavities (common Fabry Perot mode) will alter the phase of the carrier at the reflected port and generates an in-phase signal at both modulation frequencies. It is planned to use the Ω_1 in-phase signal to lock the common Fabry Perot mode.
A change of the power recycling cavity will destroy the symmetry in the two Ω_1 sidebands. One sideband will be closer to the exact resonance frequency than the other. This 'more-resonant' sideband will experience more losses in the PR-cavity than its counterpart which means that their amplitudes will be different. This difference generates a quadrature signal. Because of the different phase shifts of the carrier and the two sidebands, we will also have an in-phase component in this signal. Thus, the oscillations of the photo current at Ω_1, caused by a detuned power recycling cavity will not be 90 degrees out of phase from the oscillations which are caused by a common Fabry Perot mode error. But it is possible to tune the RF-demodulation phases to generate error signals which are at least orthogonal at the locking point.
Because the PR-cavity is usually overcoupled for the carrier, the quadrature signal changes it sign after a very small detuning of the cavity. This inversion reduces the locking range. Therefore it seems to be useful to use the quadrature component of the pick off signal for pre-locking.

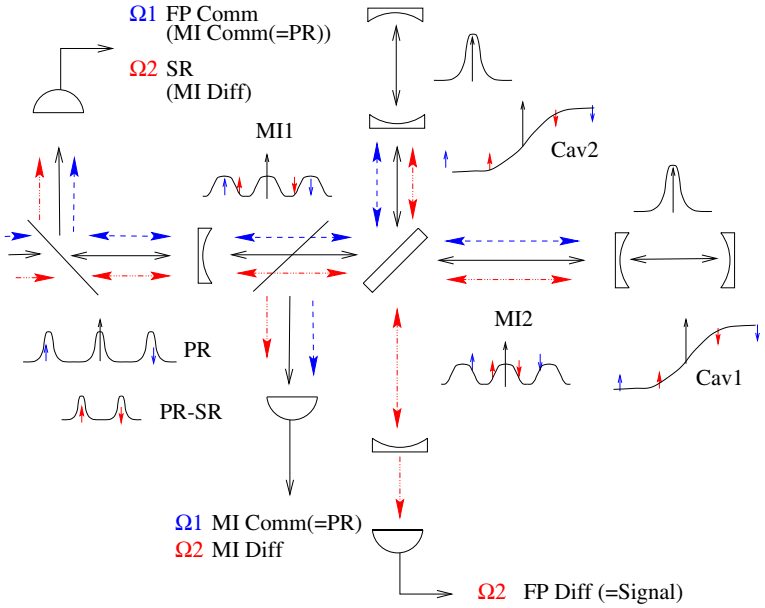

Figure 3: The locking scheme: The first modulation frequency Ω_1 will be used to lock the common Fabry Perot mode and the power recycling cavity. The second modulation frequency Ω_2 will be used to lock the differential modes (FP and MI) and the SR-PR-cavity.

A differential change of the arm cavities (differential Fabry Perot mode, i. e. the signal) will alter the interference at the beamsplitter. The dark port will not be perfectly dark anymore and after demodulation with the Ω_2 sidebands at the photodiode an in-phase signal will appear in the photocurrent. Because the second sideband is resonant in the PR-SR-cavity and MI1 is nearly bright for this sideband, its amplitude will be large compared to many other schemes. The only other longitudinal degree of freedom which generates an error signal at this port is the differential MI1 mode.
The last two degrees of freedom, the PR-SR-cavity and the differential Michelson are the most difficult parts.

One reason for the difficulty is the desired tunability of the SR-cavity; this tuning also changes the PR-SR-cavity. Another reason is the second Michelson interferometer, which tends to alter the intensities in the north and east arms. To begin, therefore, we will examine the broadband case, where the SR-cavity is on resonance and not detuned.
MI1 is nearly bright for the second sideband and in this case the PR-SR-cavity is the one in which the sideband can resonate. A change of the length of this cavity can be caused either by a change of the PR-cavity, which should be already locked, or by a change of the SR-cavity. This length change will shift the phases of the sidebands and will generate an in-phase error signal at the reflected port. MI1 acts as a frequency dependent loss mechanism for the PR-SR-cavity. A

change of MI1 will increase the losses for one sideband and reduce them for the second sideband, generating a quadrature error signal at the reflected port and also at the pick off.

5 Summary

We described a possible Modulation/Demodulation scheme to control a dual recycled cavity enhanced Michelson interferometer. A tabletop experiment has been designed and construction is nearly compleated to test this scheme.
Lock acquisition is also of interest but the results of a bench-top experiment with fixed mirror mounts will only be of limited use for a fully suspended system like LIGO II. Therefore numerical modelling of the interferometer and a fully suspended prototype experiment are the essential next steps to understand the complex behaviour of a gravitational wave detector in this configuration.

6 Acknowledgments

This work is supported by the NSF through grant PHY-9722114 .

References

1. The best sources for informations about the different gravitational wave detectors are their web-pages:
   TAMA: http://tamago.mtk.nao.ac.jp/
   VIRGO: http://www.pg.infn.it/virgo/
   LIGO: http://www.ligo.caltech.edu/
   GEO600: http://www.geo600.uni-hannover.de/
2. M. Regehr, "Signal Extraction and Control for an Interferometric Gravitational Wave Detector", CalTech Ph.D. Thesis, (1995)
3. G. Heinzel *et al*, *Phys. Rev. Lett.* **81**, 5493 (1998)